ANL/ET/CP-101896

ONE-SIDED INFRARED THERMAL IMAGING FOR FLAW CHARACTERIZATION OF CERAMIC MATRIX COMPOSITES[†]

C. Deemer, J. G. Sun, and W. A. Ellingson

Energy Technology Division
Argonne National Laboratory
Argonne, IL 60439

April 2000

Abstract submitted for presentation at the American Ceramic Society's 102nd Annual Meeting and Exposition, St. Louis, Mo, April 30- May 3, 2000.

[†]Work sponsored by the U.S. Department of Energy, Energy Efficiency and Renewable Energy, Office of Industrial Technologies, under Contract W-31-109-ENG-88.

DISCLAIMER

DISCLAIMER

Portions of this document may be illegible in electronic image products. Images are produced from the best available original document.

ONE-SIDED INFRARED THERMAL IMAGING FOR FLAW CHARACTERIZATION OF CERAMIC MATRIX COMPOSITES *

C. Deemer, J. G. Sun, and W. A. Ellingson

Energy Technology Division
Argonne National Laboratory
Argonne, IL 60439

*Work sponsored by the U.S. Department of Energy, Energy Efficiency and Renewable Energy, Office of Industrial Technologies, under Contract W-31-109-ENG-88.

ABSTRACT

One-sided infrared thermal imaging is being used to characterize voids and delaminations in SiC/SiC composites. Flaw depth is estimated by examining the decay of surface temperature after application of a thermal pulse. Digital analysis of the surface temperature/time relationship allows characterization of the sizes and positions of defects. Results show that defects of various sizes and depths can be characterized in SiC/SiC composites with the technique.

INTRODUCTION

In recent years, significant efforts has been given to development of nondestructive evaluation technology for application of continuous fiber ceramic composites (CFCCs). Current efforts in NDE are being directed towards coupling to life time prediction of these material systems. This is driving the need for more accurate flaw size and position characterization.

Delaminations are one type of flaw that has been shown to degrade the performance of CFCCs in high-temperature environments. It is known that through-thickness thermal diffusivity mapping is a reliable method of detecting and describing the sizes, shapes, and positions of these flaws[1]. However, this technique can not determine flaw depth of the flaw. Argonne National Laboratory's thermal-infrared nondestructive evaluation laboratory has developed a one-sided flash technique for measuring the depth of thermally insulating internal macroscopic flaws such as delaminations or flat-bottomed holes (the later was used in this study, to simulate delaminations). The one-sided flash technique uses an infrared focal plane array to detect the surface temperature of the specimen after a single thermal pulse has been applied to that surface. A pixel-by-pixel analysis of the decay of the surface temperature/time relationship will then determine the thickness of the sample at that position. If a thermally insulating flaw such as a delamination exists, analysis of the temperature decay will determine the depth of the flaw beneath the surface.

The technique discussed here allows automated depth measurements. Prior techniques such as described by Favro et al.[2] and Ringermacher and Archacki[3] require

that the slope of the surface temperature decay be found numerically before the depth can be determined. This causes drastic increases in signal noise. Due to the low thermal diffusivity, high surface roughness, and variations in emissivity, measurements of the transient temperature of ceramics are inherently noisy. Amplification of the noise due to the slope determination process creates great difficulties in automating these techniques. The one-sided thermal imaging technique described here does not require the slope of the temperature decay to be calculated, thereby making automation a viable option.

THEORY

To measure specimen thickness, the one-sided pulsed thermal NDE technique examines decay of the surface temperature (or cooling curve) after a thermal pulse has been applied to that surface with flash lamps. The amount of energy in the flash, material properties, and the geometry of the specimen affect the decay of the surface temperature.

To understand how the geometry affects the cooling curve, three different configurations were studied: a finite plate, a semi-infinite medium, and a point directly above a flat-bottomed hole in a semi-infinite medium, as seen in Fig. 1. The temperature of the semi-infinite medium directly after the flash is very high. As the thermal energy dissipates into the material, the temperature on the surface decays asymptotically to the temperature of the surface prior to the flash. The finite plate begins at the same high temperature after the flash and decays at the same rate as the semi-infinite medium until just before the characteristic time given by Leung and Tam[4]

$$\tau_L = L^2/\pi^2\alpha, \qquad (1)$$

where L is the thickness, and α is the thermal diffusivity. At that point, the cooling curve diverges from that of the semi-infinite medium and approaches a final temperature. This final temperature is higher than the initial temperature, as the plate only has a finite amount of material to absorb the thermal energy. The flat-bottomed hole cools at the same rate as the finite plate until the thermal energy flows laterally. When this occurs, the cooling curve diverges away from that of the finite plate, and begins to converge with the cooling curve of the semi-infinite medium.

By subtracting the cooling curves of the flat-bottomed hole and the semi-infinite medium, the time-difference curve is found. Favro et al.[2] suggested that the maximum slope (peak-slope) is a characteristic point on the time-difference curve. It has been shown that there is a linear relationship between the time when the maximum slope occurs (peak-slope time) and the squared depth of the flaw[5]. Ringermacher and Archacki[3] stated that the peak-slope time is given by

$$\tau_{PS} = 3.642\tau_L. \qquad (2)$$

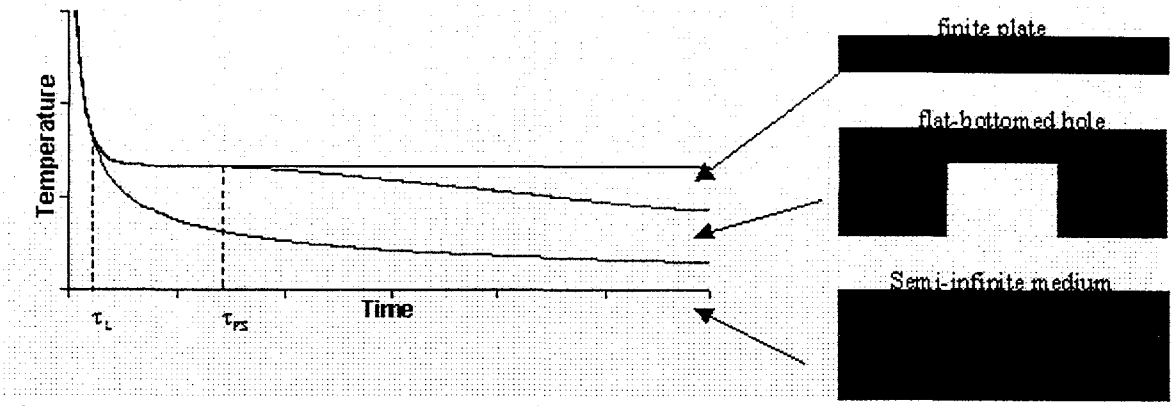

Fig. 1. Temperature decay on the flashed surface for a finite plate, a flat-bottomed hole, and a semi-infinite medium, where τ_L is the characteristic time and τ_{PS} is the peak-slope time.

Moreover the peak-slope time remains constant as the diameter of the flat-bottomed hole changes. This indicates that the cooling curve of the flat-bottomed hole has not diverged from that of the finite plate at the time τ_{PS}. Therefore, between the characteristic time and the peak-slope time, the surface temperature of a flat-bottomed hole decays as if it were in a finite plate ($\tau_L<t<\tau_{PS}$). Given the thermal diffusivity α, the measurement can be curve-fitted to the analytical solution of a finite plate after an instantaneous heat pulse where the thickness of the absorption layer is infinitely small. This is given by Parker et al.[6] as

$$T(t) = \frac{Q}{\varrho\, CL}\left[1 + \sum_{n=1}^{\infty} \exp\left(-\frac{n^2\pi^2}{L^2}\alpha\, t\right)\right], \tag{3}$$

where Q is the radiant energy absorbed into the sample, C is the specific heat, ρ is the mass density, and t is the time. The value $Q/\rho CL$ is equivalent to T_f, which is the final temperature of the finite plate.

The curve fit of the measured data to Eq. 3 is an iterative routine where given an initial guess for the thickness; the characteristic time and the peak-slope time are calculated by using Eq. 1 and 2, respectively. Then the final temperature (with the given thickness) is fitted by using a linear least-squares fit calculated from

$$T_f = \frac{\sum_{i=q}^{p}\{D_i T(t_i)\}}{\sum_{i=q}^{p} T(t_i)^2} \tag{4}$$

where q and p correspond to the frames when the characteristic time and the peak-slope time occur, respectively, D_i is the measured temperature, and t_i is the time when the i^{th} frame occurs. Now that the final temperature has been found, the new value for the thickness is derived with the Newton-Rapson technique, an iterative process in which, given the initial guess, an updated guess for the thickness is calculated from

$$L_{j+1} = L_i - \frac{\sum_{i=q}^{p}[T(t_i) - D_i]}{\sum_{i=q}^{p}\left\{\frac{\partial^2 T(t_i)}{\partial L^2}[T(t_i) - D_i] + \left(\frac{\partial T(t_i)}{\partial L}\right)^2\right\}} \quad (5)$$

Using this new value for the thickness, one can repeat the process until the change in calculated thickness is small. Note that the average squared error is minimized (i.e., squared error/number of data points fitted), unlike to the squared error used in most curve-fitting routines, because the number of data points that are fitted differs for each iteration.

EXPERIMENTAL SETUP

The thermal imaging system developed at ANL consists of an infrared camera with a 256 x 256 focal-plane array of InSb detectors, a 200 MHz Pentium-based PC computer equipped with a high-speed digital frame grabber, and a function generator that produces an adjustable frame rate for the camera. The thermal pulse is applied with a photographic flash lamp system. A dual-timing trigger is used for simultaneous triggering of the flash lamps and data acquisition. An analog video system is used to monitor the experiments.

In setting up for the front-flash measurement, the lamps are placed on the same side of the sample as the camera (see Fig. 2). When the lamps are triggered, the computer simultaneously begins acquiring a series of thermal images from the infrared camera at a preset rate. These thermal images represent the surface temperature decay as a function of time (i.e., the cooling curves) over the entire region of the viewed surface. The computer then stores the digital images on a hard disk for further processing.

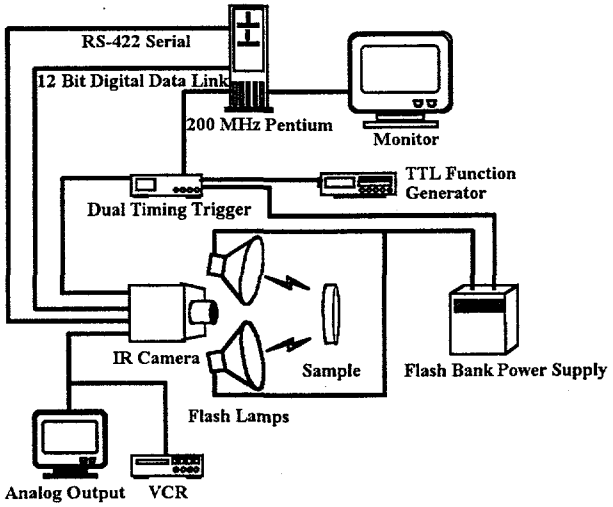

Fig. 2. Schematic diagram of thermal imaging system in front-flash setup.

RESULTS

For this study an 8-ply 8 harness satin-weave polymer-impregnated SiC/SiC CFCC flat plate was fabricated by Dow Corning Corporation. This sample uses CG-Nicalon fibers woven into an 8HS fabric and processed with polymer impregnation and pyrolysis. Flat-bottomed holes were machined into one face of this specimen (see Fig. 3). Prior to machining, through-thickness thermal diffusivity was measured in each specimen with a technique developed at ANL[1]. The results showed that the plate was relatively homogeneous, and had a thermal diffusivity of 0.97 mm^2/s, consistent with previous findings [7].

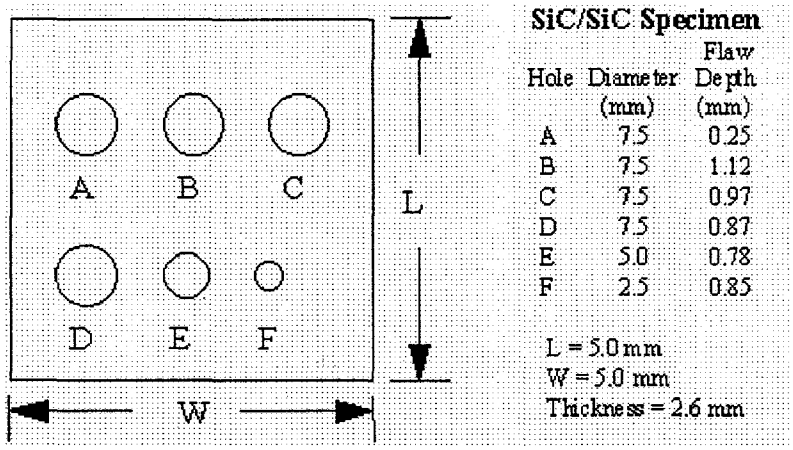

Fig. 3. Schematic illustration of the Dow Corning SiC/SiC CFCC specimens with machined flat-bottom holes.

A point above each hole was curve-fitted using the described technique. The results are given in Table I. Together with the thickness, the data were fitted to find the final temperature and the time when the flash occurred. However, discrepancies were seen in the calculated values of the flash time. This value varied from flaw to flaw, and was due to an error in the calculation of the surface temperature for times shortly after the flash. It is believed that this also caused the errors in the thickness estimation. The depth of flaw-A (0.25 mm deep, 7.5 mm diameter) could not be calculated because of the proximity of the flaw to the surface. This caused the cooling curve to reach the peak-slope time before the detector could recover from the flash.

Table I. Calculated and measured depths.

Flaw	Calculated Depth (mm)	Measured Depth (mm)
A	na	0.25
B	1.14	1.12
C	0.99	0.97
D	0.824	0.87
E	0.835	0.78
F	0.826	0.85

CONCLUSIONS

A one-sided thermal model has been developed to predict depth of defecs in ceramic composites. The curve fit is done only up to the time when the temperature of the sample diverges from that of a plate of finite thickness, thereby avoiding the effect of lateral diffusion of heat around the flaw. This allows the depth measurements to be automated to produce a depth map of an entire specimen. Results from an SiC/SiC continuous fiber ceramic composite sample with flat-bottomed holes show that the technique produces values for the depths of simulated flaws that correspond well to actual depths.

ACKNOWLEDGMENTS

This work was funded by the U.S. Department of Energy, Energy Efficiency and Renewable Energy, Office of Industrial Technologies CFCC program , under Contract W-31-109-ENG-88. The authors thank Drs. T. E. Easler and A. Szweda of Engineering Ceramics (formely with Dow Corning Corporation) for providing the test sample used in this study.

REFERENCES

[1]Stuckey, J., Sun, J. G., and Ellingson, W. A., "Rapid Infrared Characterization of Thermal Diffusivity in Continuous Fiber Ceramic Composite Components," presented at 8th Int. Symp. on Nondestructive Characterization of Materials, Boulder, CO, June 15-20, 1997.

[2]Favro, L. D., Han, X., Wang, Y., Kou, P. K., and Thomas, R. L., "Pulse-Echo Thermal Wave Imaging," in Review of Progress in QNDE, Vol. 14, Plenum Press, 1995

[3]Ringermacher, H. I., and Archacki, R. J., "Nondestructive Testing: Transient Depth Thermography," United States Patent No.: 5,711,603, Jan, 27, 1998.

[4]Leung, W. P., and Tam, A. C., "Techniques of Flash Radiometry," J. Appl. Phys., **56**[1], 153-161, 1984.

[5]Deemer, C., Sun, J. G., Ellingson, W. A., and Short, S., "Front-Flash Thermal Imaging of Continuous Fiber Ceramic Composites," presented at 23rd annual Cocoa Beach Conference & Exposition: an International Conference on Engineering Ceramics and Structures, Cocoa Beach, FL, Jan, 25-29, 1999.

[6]Parker, W. J., Jenkins, R. J., Butler, C. P., and Abbott, G. L., "Flash Method of Determining Thermal Diffusivity, Heat Capacity, and Thermal Conductivity," J. Appl. Phys., 32 [9], 1679-1684, 1961.

[7]Sun, J. G., Deemer, C., Ellingson, W. A., Easler, T. E., Szweda, A., and Craig, P. A., "Thermal Imaging Measurement and Correlation of Thermal Diffusivity in Continuous Fiber Ceramic Composites," in Thermal Conductivity 24, P. S. Gaal and D. E. Apostolescu, pp. 616-622, 1999, and presented at 24th Int. Thermal Conductivity Conf., Pittsburgh, Oct. 26-29, 1997.